Effects of doped acceptor ions on proton diffusion in perovskite oxides: a first-principles molecular-dynamics simulation

1998 J. Phys.: Condens. Matter 10 285

(http://iopscience.iop.org/0953-8984/10/2/007)

J. Phys.: Condens. Matter **10** (1998) 285–294. Printed in the UK PII: S0953-8984(98)88057-0

Effects of doped acceptor ions on proton diffusion in perovskite oxides: a first-principles molecular-dynamics simulation

Fuyuki Shimojo†, Kozo Hoshino† and Hideo Okazaki‡

† Faculty of Integrated Arts and Sciences, Hiroshima University, Higashi-Hiroshima 739, Japan
‡ Department of Physics, Faculty of Science, Niigata University, Niigata 950–21, Japan

Received 1 October 1997

Abstract. The effects of doped acceptor ions on proton diffusion in the protonic conductor Sc-doped $SrTiO_3$ are studied by means of a first-principles molecular-dynamics simulation. It is found that the proton forms an O–H bond with the neighbouring O ion, and that the frequency of the O–H stretching vibration depends on the position of the proton in the crystal. The frequencies obtained from our simulations are consistent with the experimental results obtained from the infrared-transmission spectra. It is shown that the position dependence of the O–H stretching vibration is caused by the electron density distribution in the Sc-doped $SrTiO_3$. Near the Sc ion, electrons tend to localize around each ion causing higher frequencies, while, near the Ti ion, the electron density between the Ti and O ions is larger than that in the undoped crystal, giving lower frequencies.

1. Introduction

The importance of high-temperature proton-conducting solids has been emphasized for a wide variety of electrochemical applications such as in fuel cells and hydrogen sensors. Since $SrCeO_3$-based protonic conductors, which exhibit protonic conduction at high temperatures, were discovered by Iwahara *et al* [1], several perovskite oxide solid solutions have been found to be high-temperature protonic conductors, and extensively studied experimentally with a view to applications [2]. However, the mechanism of proton migration in the materials has not yet been clarified, though there have been some attempts made [3]. The purpose of our study is to investigate, by means of a first-principles calculation, the microscopic mechanism of proton migration, including features such as stable positions, probable migration paths of protons and effects of doped acceptor ions on these properties for perovskite oxides.

Recently, Sata *et al* [4] carried out several experimental measurements in order to investigate the mechanism of large-protonic conduction in heavily Sc-doped $SrTiO_3$, which is a typical perovskite oxide. Among the perovskite oxides, this is one of the most suitable materials for studying the stable position of a proton experimentally, because its crystal structure is simple. Sata *et al* performed neutron diffraction measurements, and found that the proton is bound by the oxygen ion with the O–H distance being about 1.2 Å as if the proton makes a hydrogen bond between the two oxygen ions. They also measured the infrared-transmission spectra in the energy region of the O–H stretching vibration, and found that the absorption dip due to the O–H stretching vibration in the Sc-doped $SrTiO_3$ is

0953-8984/98/020285+10$19.50

broad and spreads over 500 cm^{-1} around the dip at 3300 cm^{-1}, while the O–H stretching energy in the undoped crystal is about 3500 cm^{-1} and is observed as a very sharp absorption dip. The broad absorption suggests that more than one stable position of the proton exists in the Sc-doped $SrTiO_3$. Sata *et al* have confirmed the high protonic conduction by means of ac-conductivity measurements.

On the other hand, there have been some theoretical attempts to clarify the mechanism of proton migration in materials [5–8]. Cherry *et al* [6] have investigated the mechanism and energetics of proton migration in a perovskite oxide, $LaAlO_3$, by means of *ab initio* quantum mechanical cluster calculations. They have optimized the geometry of the ions. In the ground state, the proton is bound to an O ion, and moves away from the Al ion, and the neighbouring O ion is drawn toward the proton. In the barrier state, in which the proton is equidistant between two adjacent O ions, both O ions are drawn toward the proton. Cherry *et al* have also calculated the energy barrier to the proton transfer as the difference in energy between the ground state and the barrier state.

More recently, Shah and co-workers [7, 8] have studied tritium diffusion in lithium oxide, which has not a perovskite structure but an antifluorite structure, by means of first-principles pseudopotential calculations. They calculated the total energies of the relaxed structures with the various positions of tritium along the supposed diffusion pathways. It has been shown that, if there is no lithium vacancy, the tritium (T) is at an interstitial site, and forms an O–T bond at a distance of about 1 Å and, furthermore, this interstitial tritium can move freely around this single O ion. Shah and co-workers proposed that the most probable migration path of the interstitial tritium is identified as a jump between the nearest-neighbour O ions. These features of tritium diffusion seem to be closely related to those of the proton diffusion in perovskite oxides investigated in this work, though the crystal structures are different.

In our previous paper [9], we studied the stable positions of a proton in Sc-doped $SrTiO_3$ by means of first-principles pseudopotential calculations. It has been shown that, in a stable ionic configuration, the position of the proton is between two neighbouring O ions, and the proton is bound to one O ion with an O–H bond length of about 1.03 Å; this looks like a hydrogen bond. This is consistent with the result of the neutron diffraction experiments reported by Sata *et al* [4] described above. The position of the proton, obtained by our calculations, is on the opposite side of the Ti (Sc) ion with respect to a line connecting the two adjacent O ions, whereas it was concluded from the experiments that it is slightly closer to the Ti-ion (Sc-ion) site. This minor difference may be caused by oxygen vacancies not being introduced in our calculations, though there are some oxygen vacancies in real materials, and by the stable positions of a proton being obtained by a steepest-descent optimization of the ionic configurations, and hence our results being concerned with zero temperature, while the experimental results include the effects of finite temperature.

So far, almost all theoretical studies on the mechanism of proton migration in materials have been carried out by calculating the energy of the system, assuming or optimizing the ionic configurations as stated above. However, to investigate the microscopic mechanism of proton migration in more detail, theoretical studies including finite-temperature effects are indispensable. In this paper, we report the results of a first-principles molecular-dynamics (MD) simulation of proton diffusion in Sc-doped $SrTiO_3$. The purposes of our MD simulation are (i) to clarify the probable migration paths of a proton, (ii) to examine the dynamic process of the proton migration in the crystal and (iii) to investigate the effects of dopant Sc ions on the proton migration. Though some of the preliminary results of our simulations have been published elsewhere [10], the effects of the dopant Sc ion on the dynamic properties of the proton have not been clarified so far. In this paper, we detail the

results of our first-principles MD simulations in investigating the microscopic mechanism of the proton diffusion in the Sc-doped $SrTiO_3$. The method of calculation is described briefly in section 2. Our work is extended for focusing on how the dopant Sc ions affect the proton migration in the crystal. The results of our simulation and a discussion are given in section 3. Finally section 4 summarizes our work.

2. The method of calculation

Our calculations are performed within the framework of the density functional theory in the local density approximation [11]. Electronic wavefunctions are expanded in the plane-wave (PW) basis set. The energy functional is minimized using an iterative scheme based on the preconditioned conjugate-gradient method [12–14].

For a conventional norm-conserving pseudopotential [15], a high PW cut-off energy is needed for systems which include first-row or transition metal elements. For this reason, in the present study, we use the ultrasoft pseudopotential proposed by Vanderbilt [16] for reducing the computational cost. The Vanderbilt pseudopotential has the following two desirable features. First, we can generate a separable pseudopotential directly without constructing a semilocal one. Second, since the usual norm-conservation constraint is removed, the pseudo-wavefunctions can be constructed so as to be as soft as possible within the core region. The atomic valence configurations treated in generating the pseudopotentials are $Sr(4s^2 4p^6 5s^1)$, $Ti(3s^2 3p^6 3d^1 4s^2)$, $Sc(3s^2 3p^6 3d^0 4s^2)$, $O(2s^2 2p^4)$ and $H(1s^1 2p^0)$.

Using the Nosé–Hoover thermostat technique [17, 18], the equations of motion are solved via the velocity Verlet algorithm with the time step $\Delta t = 0.48$ fs. The cubic supercell contains 41 atoms, $8(SrTi_{1-x}Sc_xO_3) + H$, with periodic boundary conditions. The MD simulations are carried out for two systems; i.e. for undoped $SrTiO_3$ ($x = 0$) and for Sc-doped $SrTiO_3$ ($x = 1/8$). The side of the cubic supercell is 7.81 Å, which is chosen so as to be consistent with the experimentally determined lattice constant of bulk $SrTiO_3$ [19]. Only Bloch functions at the Γ point are used. The PW cut-off energy is 25 Ryd, which gives a good convergence of the total energy. We confirmed that the lattice constant of bulk $SrTiO_3$ calculated using these parameters is in reasonable agreement with the experimental value. Several MD simulations are performed with various initial positions of the proton. Each simulation is carried out for about 1 ps and at the temperature of 1000 K. The optimized structure is used as the initial configuration of the ions. The initial charge density for each MD step is estimated by extrapolating the charge densities for the previous steps [13], and the initial wavefunctions are estimated from the wavefunctions for the previous steps by a subspace diagonalization [12].

3. Results and discussion

3.1. The electronic density of states

Using the stable ionic configuration [9], the electronic density of states (DOS) is calculated, and is shown in figure 1, where the total and the partial DOS for the Sc-doped $SrTiO_3$ are displayed. The angular momentum dependence of the DOS is calculated by projecting corresponding wavefunctions using the spherical harmonics whose centre is the position of each ion, and the peaks of each partial DOS are characterized by the angular momentum around each ion. The partial DOS for the Sr ion consists of two sharp peaks at about -34 and -16 eV, which correspond to the 4s and 4p states of Sr ion, respectively. As for the partial DOS for the Ti (or Sc) ion, two sharp peaks at about -57 (-47) and -33 (-27)

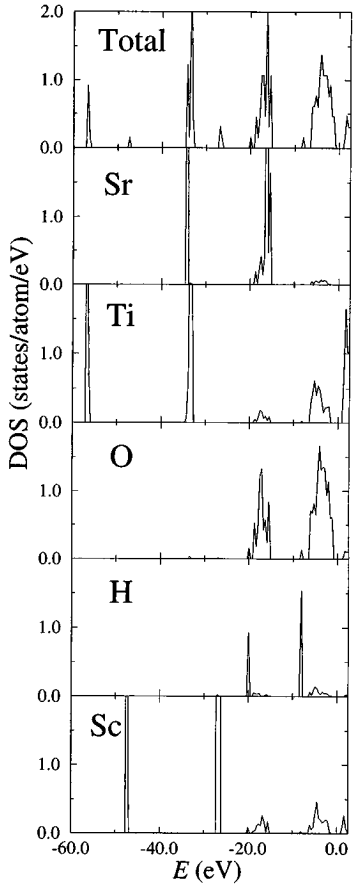

Figure 1. The total and partial electronic density of states for Sc-doped $SrTiO_3$ in which a proton is introduced in its stable position.

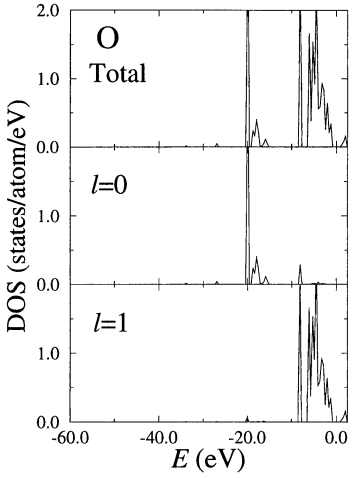

Figure 2. The partial electronic density of states for an O ion bound to a proton in Sc-doped $SrTiO_3$.

eV correspond to the 3s and 3p states of the Ti (Sc) ion, respectively, and broad peaks at about −17 and −4 eV have p and d character, respectively. The partial DOS for the O ion consists mainly of two broad peaks at about −17 and −4 eV, which have s and p character, respectively, and the broadness is caused by the 2s(O)–4p(Ti or Sc) and the 2p(O)–3d(Ti or Sc) hybridization. It should be noted that the peak of the partial DOS for the Ti ion at about −4 eV is larger than that for the Sc ion, which means that the 2p(O)–3d(Ti) hybridization is stronger than the 2p(O)–3d(Sc) hybridization. This affects the mechanism of proton migration, which will be clarified later.

There are two sharp peaks in the partial DOS for the proton at about −20 and −8 eV, and the partial DOS for the O ion has small peaks at the same energy. Since these peaks appear only in the partial DOS for the O ion bound to the proton as shown in figure 2, they are bound states related to form the O–H bond. When the DOS is calculated for the barrier state in which the proton is equidistant between two adjacent O ions, the sharp peaks of bound states appear in the partial DOS for both O ions as well as for the proton. This means that the proton is partially bonded to the two O ions. It is, therefore, probable that the proton migrates from one O ion to another with no significant bond breaking. This

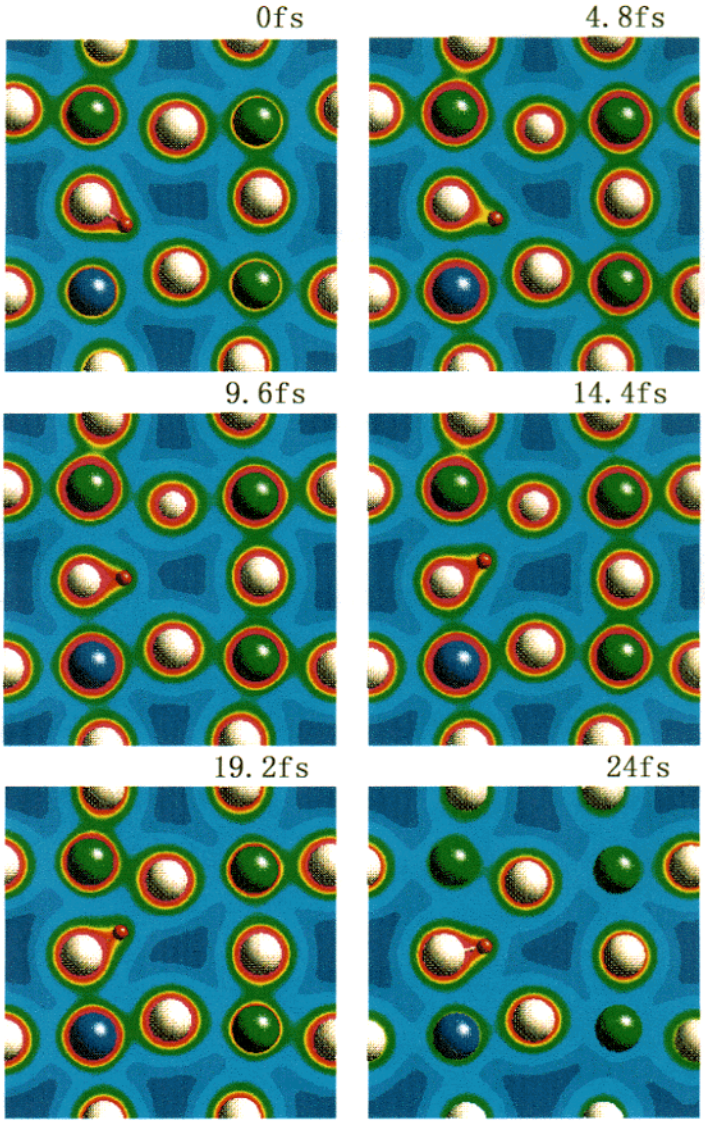

Figure 3. The time evolution of the electron density distribution $\rho(r)$ with the proton diffusion around the O ion. $\rho(r)$ is displayed in the (100) plane including the proton at each time. With increase in $\rho(r)$, the colour is changed to deep blue, blue, green, yellow and red. The small red ball shows the position of the proton, and the white, green and blue balls show the positions of the O, Ti and Sc ions, respectively.

probability will be confirmed by investigating the time evolution of the electron density distribution with the proton diffusion, as shown in the next section.

3.2. The time evolution of the electron density distribution

In our first-principles MD simulations, we observe two types of diffusion path: one is a diffusion around an O ion and the other is a diffusion between the two neighbouring O ions.

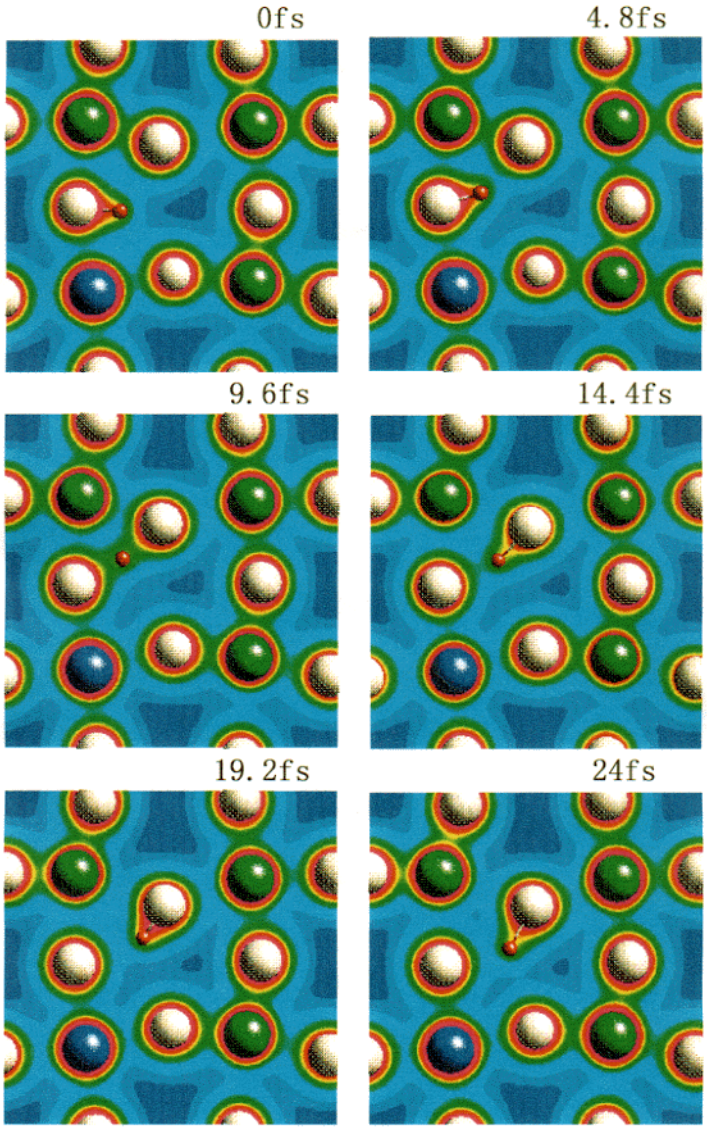

Figure 4. The time evolution of the electron density distribution $\rho(r)$ with the proton diffusion between the two neighbouring O ions. Refer to the caption of figure 3.

Figures 3 and 4 show the time evolution of the electron density distribution $\rho(r)$ for typical cases of the proton diffusion. $\rho(r)$ is displayed in the (100) plane including the proton at each time. With increasing $\rho(r)$, the colour is changed to deep blue, blue, green, yellow and red. The small red ball shows the position of the proton, and the white, green and blue balls show the positions of the O, Ti and Sc ions, respectively. As shown in figure 3, the proton, which stays in a stable position and is bound to an O ion at $t = 0$ fs, migrates around the O ion from site to site. It is found that the time required for this process is about 20 fs, and the O–H bond is retained during the migration. On the other hand, we can see, from figure 4, that the proton migration between the two neighbouring O ions occurs

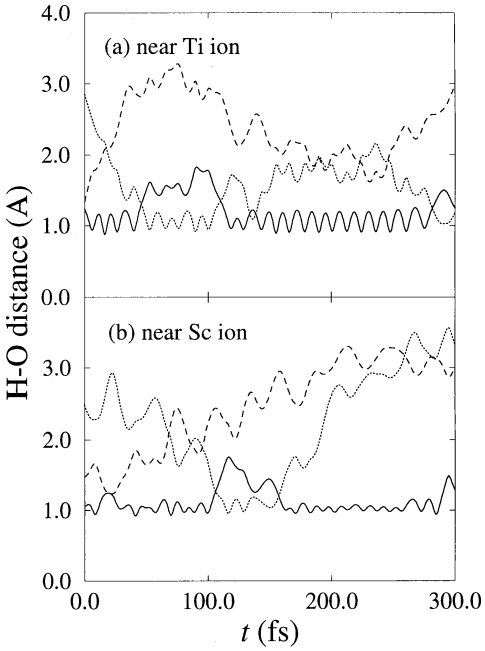

Figure 5. The time evolution of the O–H distances (a) near a Ti ion and (b) near a Sc ion for $t = 300$ fs. In each figure, the distances between the proton and the first-, the second- and the third-neighbour O ions at $t = 0$ fs are shown by solid, dashed and dotted lines, respectively.

while switching the O–H bond, and in a shorter time, i.e. less than 10 fs in this case. As expected, the situation in which the proton is partially bonded to two adjacent O ions is actualized in dynamic simulations as displayed in the figure at $t = 9.6$ fs.

3.3. The microscopic mechanism of proton diffusion

In order to investigate the proton diffusion in more detail, we calculate the distance between the proton and each O ion as a function of time. Figure 5 shows the time evolution of the O–H distances for 300 fs for the proton (a) near the Ti ion and (b) near the Sc ion in the Sc-doped $SrTiO_3$. The proton is considered to be near the Ti ion or near the Sc ion when it is bound to an O ion which neighbours two Ti ions or at least one Sc ion, respectively. In each panel, the distances between the proton and the first-, the second- and the third-neighbour O ions at $t = 0$ fs are shown by the solid, dashed and dotted lines, respectively. The origin of time does not correspond to the start of the simulation. The small oscillation at around 1 Å corresponds to the O–H stretching vibration, and the proton diffusion is recognized by a gradual increase or decrease of the O–H distances. It is found from these figures that the proton migration between the two neighbouring O ions accompanied by switching of the O–H bond occurs frequently in the Sc-doped crystal, i.e. at $t = 50$, 110, 130 and 280 fs in figure 5(a) and at $t = 20$, 110 and 160 fs in figure 5(b). In the simulation for the undoped crystal, this type of migration seldom occurs. Therefore, it is considered that, in the Sc-doped crystal, the O–H bond becomes weak because of the presence of the acceptor ions, and the proton migrates more easily as compared with the case for the undoped crystal.

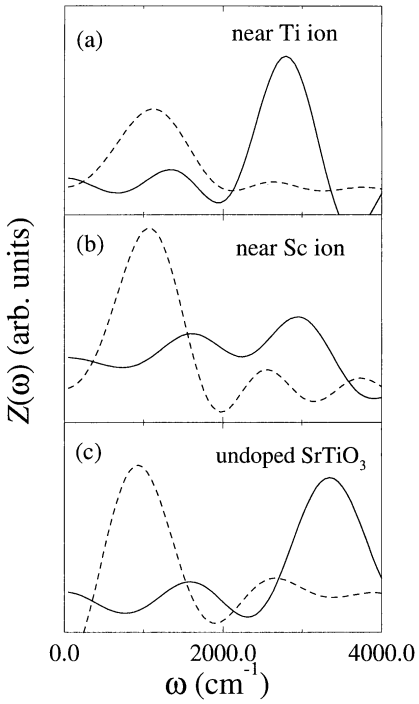

Figure 6. The power spectrum $Z(\omega)$ of the velocity–velocity autocorrelation function of the proton; (a) $Z(\omega)$ for the proton near a Ti ion, (b) $Z(\omega)$ for the proton near a Sc ion in Sc-doped $SrTiO_3$ and (c) $Z(\omega)$ for the proton in undoped $SrTiO_3$. In each panel, the solid and dashed lines correspond to stretching and bending motion, respectively.

It should be noted that the O–H stretching vibration continues during the proton diffusion near both the Ti and Sc ions, and the amplitude of the vibration near the Ti ion is larger than that near the Sc ion. To investigate the frequency distribution of the vibrating motion, the velocity–velocity autocorrelation function $Z(t)$ and its power spectrum $Z(\omega)$ are calculated for the proton. It is found that $Z(\omega)$ is mainly characterized by two peaks at low frequency (about 1000 cm^{-1}) and high frequency (about 3000 cm^{-1}). We separate the velocity of the proton into two components, parallel and perpendicular to the O–H bond, and calculate $Z(t)$ for each component so as to identify each peak of $Z(\omega)$. Figures 6(a) and 6(b) show the spectrum $Z(\omega)$ of the proton near the Ti ion and near the Sc ion, respectively, for the Sc-doped $SrTiO_3$. For comparison, the spectrum $Z(\omega)$ of the proton in the undoped $SrTiO_3$ is shown in figure 6(c). In each panel, the solid and dashed lines correspond to stretching and bending motions, respectively. We note that the $Z(t)$ obtained by our simulations have some oscillations at large t, since the simulation time is not long enough for us to obtain the time-correlation functions precisely. This affects mainly the peak widths of the spectrum $Z(\omega)$ and, therefore, we discuss its peak positions only. From these figures, we can see that the frequency of the O–H stretching vibration is about 2800 and 3000 cm^{-1} near the Ti and Sc ions, respectively, while it is about 3400 cm^{-1} in the undoped $SrTiO_3$. These results are consistent with the infrared-transmission measurement of Sata *et al* [4]. They have found that the absorption of the O–H stretching in Sc-doped $SrTiO_3$ is very broad, which suggests that more than one stable position of the proton exists in the Sc-doped crystal. It is clarified that the broad absorption observed is due to the site dependence of

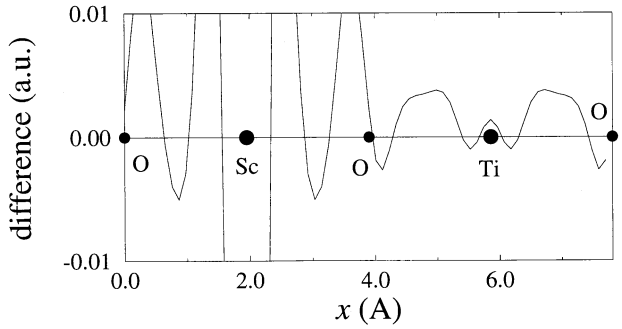

Figure 7. The difference of the electron charge densities $\rho(r)$ of undoped and Sc-doped $SrTiO_3$. The difference along the (100) line including Ti, Sc and O ions is shown. The positive values mean that $\rho(r)$ for the Sc-doped crystal has larger values than that for the undoped crystal.

the O–H stretching vibration. The frequency 3400 cm^{-1} for the undoped crystal is larger than that for the Sc-doped crystal and is in good agreement with the experimental value, 3500 cm^{-1} [4].

As clarified above, the proton diffusion near the dopant Sc ion is clearly different from that near the Ti ion. To investigate an origin of this difference, we calculate the difference of the electron charge densities $\rho(r)$ of the undoped and Sc-doped $SrTiO_3$, in which the proton is not introduced to avoid complexity. Figure 7 shows the difference of the $\rho(r)$ along the (100) line including the Ti, Sc and O ions, where positive values mean that the $\rho(r)$ for the Sc-doped crystal has larger values than that for the undoped crystal. It is found that, for the Sc-doped crystal, there is a tendency for $\rho(r)$ to localize around the Sc ion and its neighbouring O ions while $\rho(r)$ between the Ti and O ions is larger than that in the undoped crystal. The electron localized around the O ion near the Sc ion will make the O–H bond stronger. This causes the frequency of the O–H stretching vibration near the Sc ion to be higher than that near the Ti ion.

4. Summary

In this paper, we have detailed our investigations into the microscopic mechanism of proton diffusion in Sc-doped $SrTiO_3$ by means of a first-principles molecular-dynamics simulation. Two types of diffusion path are observed; one is the diffusion around an O ion while retaining the O–H bond and the other is the diffusion between two neighbouring O ions while switching the O–H bond. During the former type of diffusion, the O–H stretching vibration proceeds and the length of the O–H bond is almost unchanged. The latter type of diffusion occurs frequently and quickly. The time evolution of the electron density distribution with the proton diffusion is investigated in detail. It is found that the proton almost always forms an O–H bond with the neighbouring O ion, and the frequency of the stretching vibration of the O–H bond depends on the position of the proton in the crystal. The frequencies are about 2800 cm^{-1} and 3000 cm^{-1} near the Ti ion and the Sc ion, respectively, in the Sc-doped $SrTiO_3$, whereas the frequency is about 3400 cm^{-1} in the undoped $SrTiO_3$. These values are consistent with the experimental results obtained from the infrared-transmission spectra. It is shown that the position dependence of the O–H stretching vibration is caused by the electron density distribution in the Sc-doped $SrTiO_3$. Near the Sc ion, electrons tend to localize around each ion causing the higher frequency,

while, near the Ti ion, the electron density between the Ti and O ions is larger than that in the undoped crystal, giving the lower frequency.

Acknowledgments

This work was supported by a Grant-in-Aid for Scientific Research on Priority Areas (No 260) from The Ministry of Education, Science, Sports and Culture, Japan. We are grateful to Professor M Ishigame for continuous encouragement and to Dr N Sata for useful discussions. We wish also to thank Professor T Oguchi for useful discussions. We also wish to thank the Computer Centre of the Institute for Molecular Science, Okazaki National Research Institutes, Japan, for the use of the NEC SX-3/34R supercomputer.

References

[1] Iwahara H, Esaka T, Uchida H and Maeda N 1981 *Solid State Ion.* **3/4** 359
[2] Iwahara H 1992 *Proton Conductors: Solids, Membranes and Gels—Materials and Devices* ed P Colomban (Cambridge: Cambridge University Press) p 122
[3] Kreuer K D 1996 *Chem. Mater.* **8** 610
[4] Sata N, Hiramoto K, Ishigame M, Hosoya S, Niimura N and Shin S 1996 *Phys. Rev.* B **54** 15 795
[5] Bates J B, Wang J C and Perkins R A 1979 *Phys. Rev.* B **19** 4130
[6] Cherry M, Islam M S, Gale J D and Catlow C R A 1995 *Solid State Ion.* **77** 207
[7] Shah R, De Vita A and Payne M C 1995 *J. Phys.: Condens. Matter* **7** 6981
[8] Shah R, De Vita A, Heine V and Payne M C 1996 *Phys. Rev.* B **53** 8257
[9] Shimojo F, Hoshino K and Okazaki H 1996 *J. Phys. Soc. Japan* **65** 1143
[10] Shimojo F, Hoshino K and Okazaki H 1997 *J. Phys. Soc. Japan* **66** 8
[11] Ceperley D M and Alder B J 1980 *Phys. Rev. Lett.* **45** 566
Perdew J P and Zunger A 1981 *Phys. Rev.* B **23** 5048
[12] Arias T A, Payne M C and Joannopoulos J D 1992 *Phys. Rev.* B **45** 1538
[13] Kresse G and Hafner J 1994 *Phys. Rev.* B **49** 14 251
[14] Shimojo F, Zempo Y, Hoshino K and Watabe M 1995 *Phys. Rev.* B **52** 9320
[15] Hamann D R, Schlüter M and Chiang C 1979 *Phys. Rev. Lett.* **43** 1494
[16] Vanderbilt D 1990 *Phys. Rev.* B **41** 7892
[17] Nosé S 1984 *Mol. Phys.* **52** 255
[18] Hoover W G 1985 *Phys. Rev.* A **31** 1695
[19] Wyckoff R W G 1964 *Crystal Structures* vol 2 (New York: Interscience)